Platinum electrochemistry through a magnifying glass

Jacobse, L.

5 The reactivity of platinum microelectrodes

Decades of catalyst research have led to the development of more and more highly active electrocatalysts. To study catalysts with large kinetic rate constants, without being hindered by the used setup, it is necessary to use specialized experimental approaches. Ultramicroelectrodes (UMEs), which have at least one dimension that is smaller than the diffusion layer thickness (≃ 10 μm) but much larger than the double layer thickness (10-100 Å), are typically used to overcome limitations by mass transport and resistance. However, the customary method of UME characterization via outer sphere redox probing has serious limitations. Here, we demonstrate these shortcomings by studying outer sphere redox couples, blank voltammetry, and various catalytic reactions for platinum UMEs. A comparison to macroscale Pt electrodes shows that UMEs perform much worse for surface sensitive catalytic reactions. Our results indicate that UME data should always be accompanied by blank characterization and reactivity measurements should be interpreted extremely carefully.

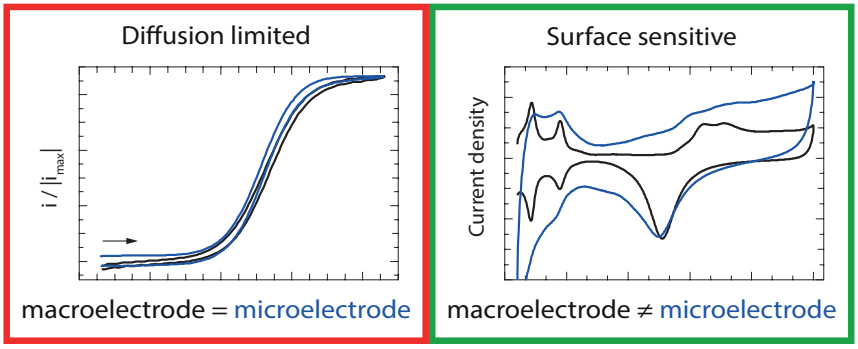

This chapter is based on Jacobse, L., Raaijman, S.J. & Koper, M.T.M. *Phys. Chem. Chem. Phys.* **18**, 28451–28457 (2016).

Electrode miniaturization increases mass transport and decreases absolute currents, both of which are beneficial for situations where high kinetic rates are concerned.[1,2] So long as the electrode is not reduced to nanometer scale, it should be possible to directly compare their results to the macro scale world. Upon further size reduction, e.g. in the case of nanoparticles, there are plenty of examples of size dependent reactivity due to the presence of specific nanoscale effects.[3–13]

On a different note, it is known from literature that the selectivity of Pt for the reduction of O_2 to H_2O (with H_2O_2 as intermediate/sideproduct) decreases by increasing the mass transport rate.[14,15] These observations were attributed to the competition between the adsorption/desorption of H_2O_2 and trace contaminants that are present even in the highest purity grade chemicals.[14–16] Furthermore, the results presented in Chapter 4 seem to indicate, unexpectedly, that already on the micrometer scale differences in catalytic reactivity can be observed for the oxidation of hydrazine on Pt electrodes in $HClO_4$.[17] This effect cannot be explained by competitive adsorption/desorption as no stable intermediates are known for the hydrazine oxidation to N_2.[18,19] These results call for a more in-depth comparison between the reactivity of platinum macroscale electrodes and UMEs.

As reviewed by Climent and Feliu, the characterization of platinum surfaces in electrochemistry is, for historical reasons, most often performed in dilute sulfuric acid.[20] In this medium, the defining features in cyclic voltammograms (CVs) are clearly visible and relatively well understood.[21] With the introduction of flame annealing, these so-called blank CVs (blanks) have enjoyed excellent reproducibility between different labs, making it the default method for electrode characterization. From such blanks, one can descern the presence/absence of contaminating species and specific reaction sites as used in Chapter 3.[20,22]

Even though such practices are now widespread within the community studying Pt electrochemistry, blank CVs of (Pt) UMEs are rarely published and if at all only for high potential scan rates[23–26] which makes them rather unsensitive towards slow reactions. Features resulting from reactions with slow kinetics or reactions which are diffusion limited (e.g. trace contaminations) will be suppressed under these conditions. Instead, surface probes such as the $[Fe(CN)_6]^{4-/3-}$ or $[FcCH_2OH]^{0/1+}$ redox couple are commonly used to characterize UMEs.[27–30] The problem is that such outer sphere redox couples are, despite some known complications[31,32], in general insensitive to surface structure, composition, and cleanliness.[33] The main benefits from these experiments are to determine electrical contact and gain information regarding the geometrical dimensions of the electrode,[1,2] but their suitability for assessing surface reactivity is highly debatable.

In this chapter, we use outer sphere redox couples, blank voltammetry, and catalytic (inner sphere) reactions to make a solid comparison between the measured catalytic reactivity of macroelectrodes and UMEs. The redox couples studied are the oxidation of ferrocenemethanol ($[FcCH_2OH]^{0/1+}$) and the reduction of hexaammineruthenium ($[Ru(NH_3)_6]^{3+/2+}$). Similarly, catalytic reduction and oxidation reactions are also studied. For catalytic reactions, we make another distinction: reactions that are well-catalyzed by Pt in general (largely surface insensitive), and reactions that are sensitive to the presence of specific surface sites ('defects'). The chosen reactions are the oxidation of hydrazine (N_2H_4),[17,18,34,35] the oxidation of methanol (CH_3OH),[12,36–40] and the reduction of nitrate (NO_3^-).[41–43] For each of these reactions, the Tafel slope, onset potential, and specific activity (where applicable) are compared to the values obtained on flame-annealed platinum electrodes under similar experimental conditions. In these experiments, we employ home-made UMEs. Information on their preparation and general experimental details can be found in Appendix F.

5.1 Electrode characterization

Outer sphere reactions

The performance of UMEs is typically demonstrated using a reversible redox couple and this is thus our starting point. Figure 5.1 shows the CV of the reduction of 1 mM $[Ru(NH_3)_6]^{3+}$ (A) and the oxidation of 1 mM $FcCH_2OH$ (B) in 0.1 KCl for a Pt UME (red) and macroelectrode (black). The voltammetry of the macroelectrode is measured in hanging meniscus configuration rotating at 2800 r.p.m. with a scan rate (ν) of 50 mV·s^{-1}. As the hysteresis in the CV of the UME is higher than for the macroelectrode, $\nu = 10$ mV·s^{-1} is used instead of $\nu = 50$ mV·s^{-1}. It should be noted that it is experimentally impossible to rotate the macroelectrode at speeds where the mass transfer coefficients would be the same for both experiments (ca. 17.000 r.p.m.). This explains the slightly less steep current increase for the macroelectrode. Apart from that no significant differences are observed between the different electrodes. Now, it is tempting to conclude that these CVs represent good and clean UMEs. However, in the following, we will demonstrate that this is not necessarily the case.

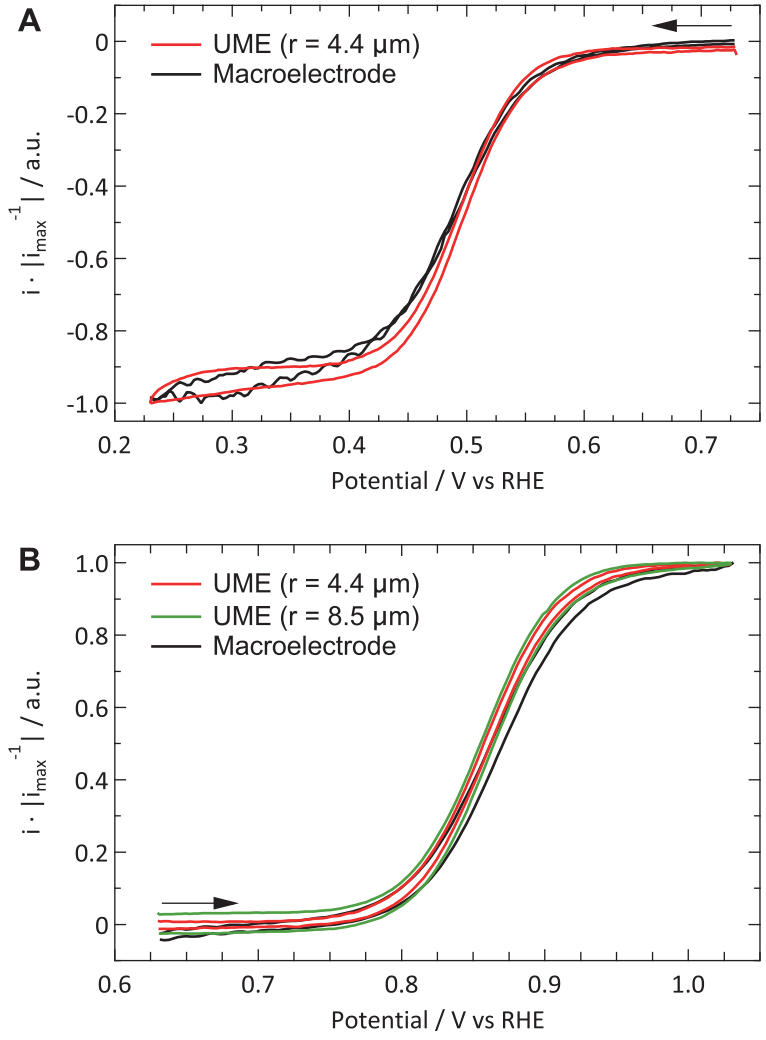

Fig. 5.1 | Characterization by outersphere reactions: **(A)** Reduction of 1 mM $[Ru(NH_3)_6]^{3+}$ **(B)** Oxidation of 1 mM $FcCH_2OH$. The supporting electrolyte is 0.1 KCl and the shown CVs are the first cycles. The potential scan rate for the UME is $\nu = 10$ mV·s^{-1}. The macroelectrode CVs are measured in hanging meniscus configuration (f = 2800 r.p.m.), with a scan rate of $\nu = 50$ mV·s^{-1}. The response of a second UME in a separate experiment under identical conditions is shown in (B).

Blank voltammetry

Outer sphere redox couples are very useful to study the geometric properties (i.e. size and shape) of an electrode. However, since they are insensitive to both surface structure and composition, they should not be the only method used to characterize a UME. Blank voltammetry is an essential tool for a full characterization, especially in the case of platinum electrodes as its voltammetric features are relatively well understood. Nevertheless, blank CVs for Pt UMEs are rarely reported and typically only at scan rates of at least $\nu = 200$ mV·s^{-1}.[23–26]

Figure 5.2 shows a decent blank voltammogram for a Pt UME (in red) compared to a flame annealed macroelectrode (in black). Although one would expect these CVs to be the same, there are some obvious differences. The hydrogen adsorption and desorption peaks (around 0.12 and 0.27 V) of the UME are not as well defined and less reversible than in the case of the macroelectrode. Also, the most negative adsorption/desorption (ca. 0.12 V) peak should be larger than the second peak (ca. 0.27 V), which it is not. The latter could in principle be explained by the production process of the thin Pt wires from which the UMEs are made. This process is known to lead to a preferential grain orientation.[44] Due to the small size of a UME, it is likely that only a single grain is exposed at the surface. Thus, the electrode can be considered to be a high-index single crystal. However, this mainly influences the ratio between the different hydrogen-related peaks and to a much smaller extent their sharpness.[22] However, this broadness might be caused by the fact that the UMEs have a relatively large roughness, as similar observations were made in Chapter 3 for the roughened Pt(111) surface.

The electrochemically active surface area of all electrodes is calculated from the hydrogen desorption integral in the region $0.06 < E < 0.6$ V after subtraction of the double layer contribution, using the recently revisited value of 230 μC·cm^{-2} for a polycrystalline Pt surface in sulfuric acid.[45] After normalization to current densities, the UMEs typically show a larger double layer (DL) current than the macroelectrodes. One could explain this by an underestimation of the surface area of UMEs due to the less well-defined hydrogen desorption features. However, this seems in contradiction with the observation that the oxide reduction peak (ca. 0.78 V) is typically smaller for the UME than for the macroelectrode. Besides the larger DL current, one could argue that there is an additional, small, peak present around 0.45 V in the negative-going scan. Finally, the shape of the platinum oxidation region usually does not clearly show two bumps, in fact showing very few identifying features at all.

The second UME blank voltammetry (green) that is shown in Fig. 5.2 demonstrates the superiority of electrode characterization using blank voltammetry instead of an outer sphere redox couple. This blank has been measured prior to the oxidation of $FcCH_2OH$ shown in Fig. 5.1B (green curve). Whereas the $FcCH_2OH$ data suggests that this electrode performs well, this is contradicted by the blank voltammetry. In this case our normalization procedure (using the hydrogen desorption area) clearly leads to an underestimate of the active surface area, resulting in much too high current densities for hydrogen adsorption, oxide formation, and DL charging. Obviously, the shape also deviates significantly from what it should be. This implies that there is a process inhibiting the hydrogen desorption and oxide reduction reactions without a significant impact on outer sphere redox chemistry.

The aim of this chapter is not to obtain the perfect blank CV of a Pt UME, but merely to provide a better insight in the reliability of currently available methods to study UMEs. Within this framework, the blank shown in Fig. 5.2 (red curve) is among the best, in terms of quality and reproducibility, that we obtained. Therefore, this is considered a good starting point to study catalytic reactions. It is expected that the underestimation of the active surface area due to a blocking process also occurs, to some extent, for the other electrodes. To prove that this has only a minor effect on the observed differences, the blank CVs measured prior to the hydrazine and methanol oxidation are shown in Fig. 5.3. The blank CV measured prior to the nitrate reduction is shown in Fig. 5.6. From these blanks it is clear that the error in determining the active surface area is always smaller than a factor of 2.

5.2 Catalytic reactivity

Hydrazine oxidation

Figure 5.4 compares the catalytic activity of a Pt UME and macroelectrode for the oxidation of 1 mM hydrazine in 0.5 M H_2SO_4 with $\nu = 50$ mV·s^{-1}. The macroelectrode shows catalytic behavior that compares favorably with reports of Álvarez-Ruiz et al.,[35] whereas the behavior of the microelectrode does not agree with the UME (r = 25 μm) results of Aldous and Compton.[34] The results obtained for the oxidation 1 mM hydrazine in this work show activity akin to the most active cycle from the 10 mM hydrazine experiments by Aldous and Compton. Also, activation of the electrode as they observe when scanning to more oxidative potentials was

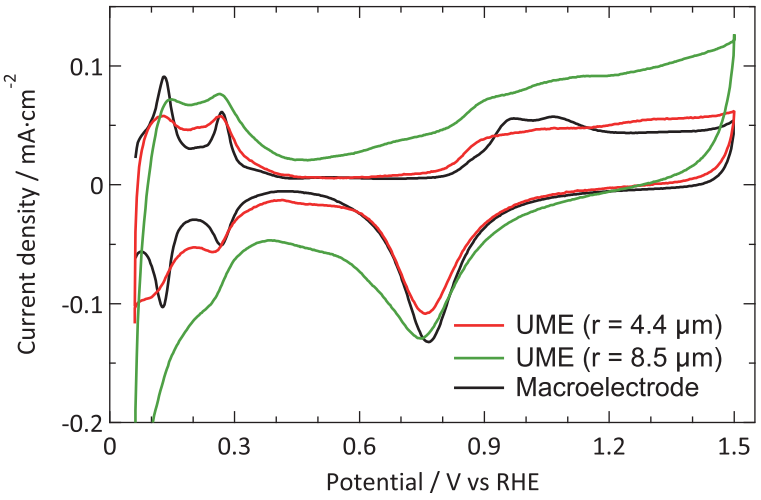

Fig. 5.2 | Characterization by blank voltammetry: Comparison of the blank voltammetries of platinum UMEs and a flame-annealed platinum spiral. The supporting electrolyte is 0.5 M H_2SO_4 and the potential scan rate is $\nu = 50$ mV·s^{-1}.

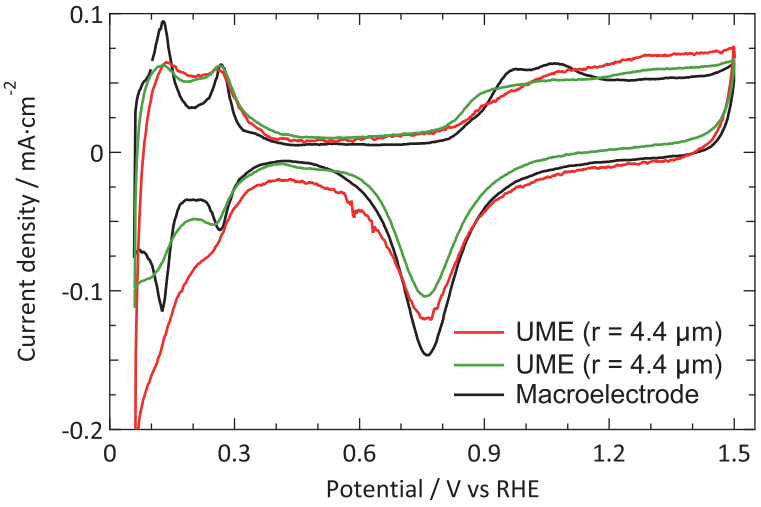

Fig. 5.3 | Blank CVs before catalytic experiments: blank CVs ($\nu = 50$ mV·s^{-1}) of a platinum UME (r = 4.4 µm) prior to the oxidation of 1 mM hydrazine (red) and 0.5 M methanol (green) in 0.5 M H_2SO_4. As the macroelectrode blanks were virtually identical, only one CV is shown (black).

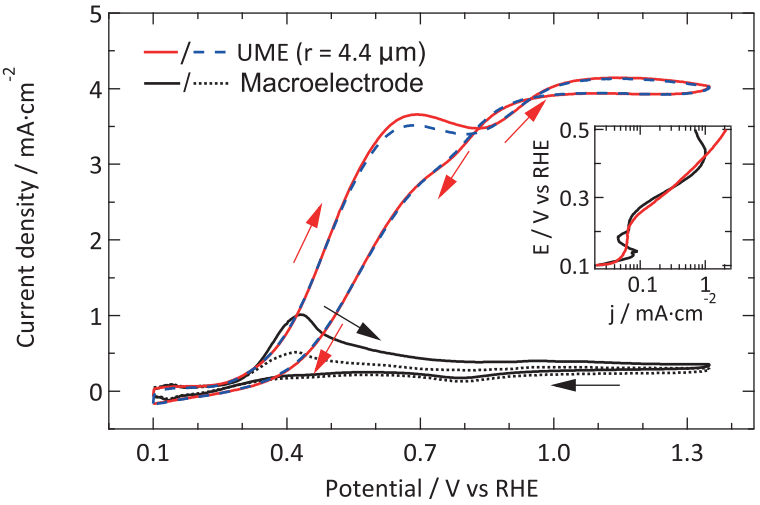

Fig. 5.4 | Hydrazine oxidation: First and fourth CV ($\nu = 50$ mV·s^{-1}) of the oxidation of 1 mM N_2H_4 in 0.5 M H_2SO_4 on a Pt UME (red and dashed blue respectively) and macroelectrode (full and dotted black line respectively). The inset shows a Tafel plot of the first anodic scans.

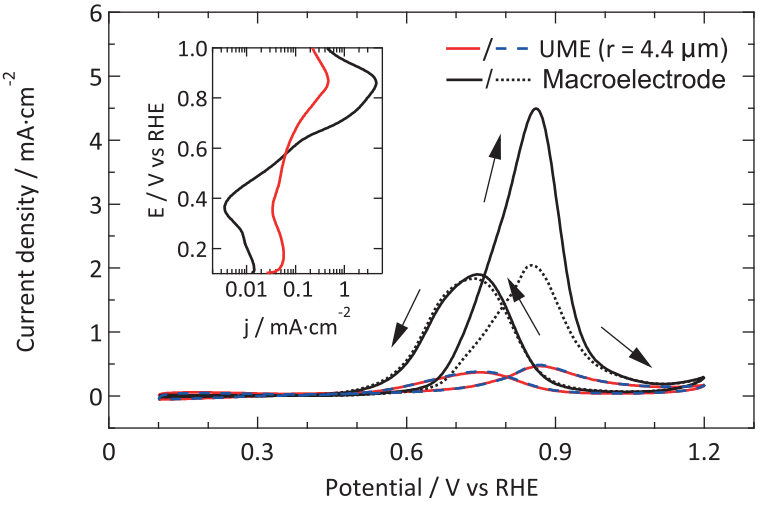

Fig. 5.5 | Methanol oxidation: First and fourth CV ($\nu = 50$ mV·s^{-1}) of the oxidation of 0.5 M methanol in 0.5 M H_2SO_4 on a Pt UME (red and dashed blue respectively) and macroelectrode (full and dotted black line respectively). The inset shows a Tafel plot of the first anodic scans.

not observed in the present study. An explanation for these differences can be found in the blank CV which is rather featureless for the data published by Aldous and Compton. Furthermore, no activation was observed when the polished microelectrode was kept at -0.05 V vs. RHE for 5 minutes prior to measuring hydrazine oxidation. These observations suggest that the activation process is rather caused by the surface becoming cleaner with cycling than by the presence of residual oxides, as suggested previously.

As Pt is a very good catalyst for the oxidation of hydrazine, a diffusion limited current is observed for both electrodes. Due to the different diffusion geometries, the CVs of the macro- and microelectrode seem to be very different at first sight. However, if one takes a closer look at the characteristic features such as the onset potential and Tafel slope, it can be concluded that both electrodes show almost the same reactivity. The only (minor) difference regarding catalytic activity is the fact that the change in Tafel slope is slightly higher for the UME than for the macroelectrode. However, as the current density is limited by the diffusion of hydrazine to the surface and not by the catalytic properties of the working electrode for most of the potential range studied, it is to be expected that both electrodes show a similar behavior. Actually, this result is more or less similar to the observations for outer sphere reactions discussed above.

Methanol oxidation

Figure 5.5 shows the catalytic activity of a Pt UME and macroelectrode towards the oxidation of 0.5 M methanol in 0.5 M H_2SO_4 with $\nu = 50$ mV·s^{-1}. Contrary to hydrazine oxidation, methanol oxidation depends strongly on the catalytic reactivity of specific Pt sites.[35,38] As we are not hindered by diffusion limitations, the CVs are similarly shaped. Moreover, this shape is in line with previous results available in literature,[39,40] although the ratio between peak currents during the forward and backward scan does not always agree. However, as this ratio is known to depend on scan rate,[40] this behavior is not completely unexpected.

Comparing the absolute reactivity, it is very clear that the UME is much less active than the macroelectrode. The good agreement between the normalized blank CVs (Fig. 5.3) confirms that this large difference (about a factor 10) cannot be explained by an error in the calculated surface areas. Furthermore, although the onset potential seems similar, the higher Tafel slope in the case of the microelectrode masks the precise onset potential.

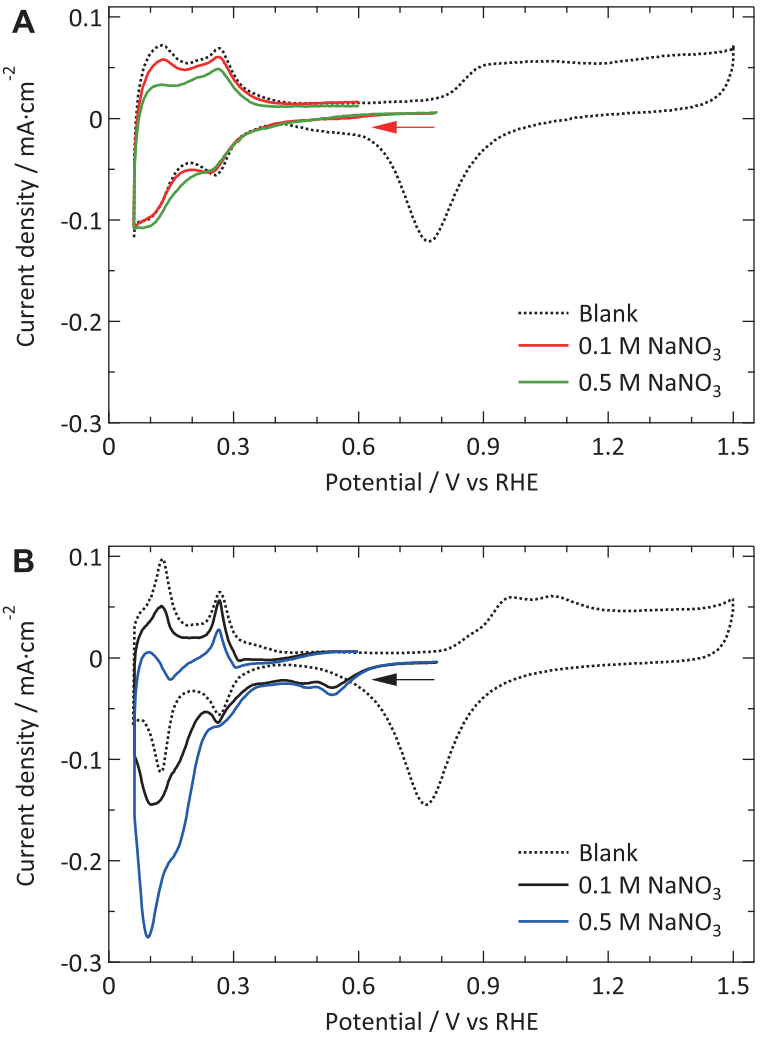

Fig. 5.6 | Nitrate reduction: Cyclic voltammetry ($\nu = 50$ mV·s^{-1}) of the reduction of 0.1 and 0.5 M nitrate in 0.5 M H_2SO_4 on **(A)** a Pt UME (red and green respectively) and **(B)** macroelectrode (black and blue respectively). The dotted lines show the blank voltammetries measured right before the nitrate reduction experiment. The same scale is used for both graphs.

Nitrate reduction

Figure 5.6 shows the catalytic activity of a Pt UME (A) and macroelectrode (B) for the reduction of 0.1 and 0.5 M nitrate in 0.5 M H_2SO_4 with $\nu = 50$ mV·s^{-1}. The corresponding blanks are shown together with the nitrate reduction experiments, to give a better indication of the current that is actually related to nitrate reduction. As nitrate reduction overlaps with hydrogen adsorption/desorption, the Tafel plots of these experiments do not provide additional insight. For the macroelectrode, the results are similar to the observations in literature.[41] However, the current for the UME deviates barely from its blank response. As the UME shows so little reactivity, nothing sensible can be said about the onset potential.

One additional remark should be made regarding the voltammetric features that the regular-sized platinum electrode shows in the region $0.5 < E < 0.6$ V vs. RHE. These peaks are likely due to the fact that the starting potential is relatively positive, and is actually also present on the microelectrodes after keeping the starting potential at 0.8 V vs. RHE for 5 seconds prior to measuring the CV. Considering that the indirect nitrate reduction starts at 0.8 - 0.9 V,[41] keeping the potential at 0.8 V for some time possibly introduces some nitrite near the surface, which could explain this additional feature observed.

5.3 UME vs. macroelectrode

In general, we can summarize the data for the catalytic reactions as exhibiting the same features as the outer sphere and blank results. Reactions that are relatively insensitive to the arrangement of the surface atoms (or their very nature) show the same reactivity for UMEs and macroelectrodes. However, for slow, more structure-sensitive reactions the UMEs are outperformed by macroelectrodes. The data suggest that the difference does not lie in the onset potential, but in the absolute current density. Also, from the blanks there is no solid evidence that a preferred grain orientation causes these differences. Thus, the most likely explanation is that part of the surface is blocked by contaminant species. As the most reactive sites will typically also bind strongest to contaminants*, it makes sense that the largest effect is observed for slow, strongly catalytic reactions that occur preferentially at these sites.

* When using platinum electrodes, methanol oxidation favors 'defect' sites and nitrate reduction is known to be very sensitive to coadsorbing species.[3]

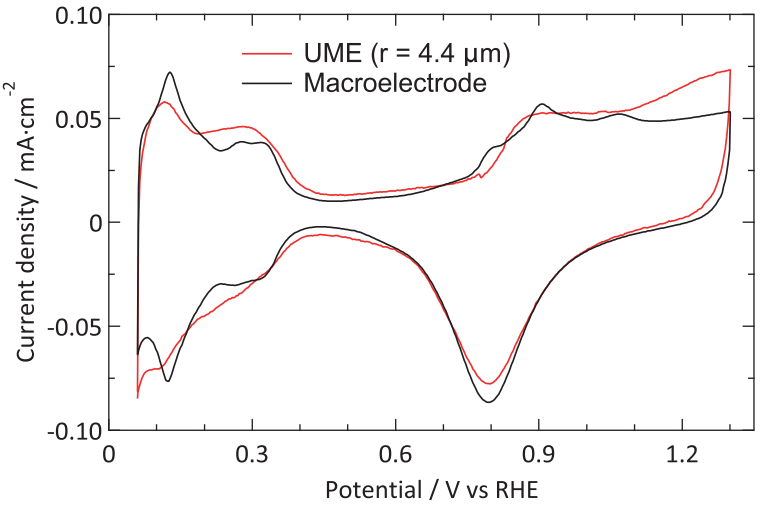

Fig. 5.7 | Characterization in $HClO_4$: Blank CVs ($\nu = 50$ mV·s^{-1}) of a platinum UME and macroelectrode in 0.1 M $HClO_4$.

A crucial distinction lies in the source of the contamination: is it introduced during the preparation/cleaning of the UME, or are UMEs much more sensitive due to faster diffusion and smaller surface area as compared to macroelectrodes. Significantly, no improvement was observed after cleaning the UME with an O_2 plasma. Thus, if UMEs are inherently contaminated to a larger degree because flame-annealing is not an option, the source of the contamination is probably not organic in nature.

Even though the cleanest chemicals available in our lab were used, the level of contamination might be relevant on this scale. For example, the sulfuric acid used (Fluka, for trace analysis) contains, according to the manufacturer's specifications, among others, ≤ 0.1 mg/kg Cl^- ions. Assuming the maximum concentration, this means that our 0.5 M H_2SO_4 electrolyte contains $1.41 \cdot 10^{-7}$ M chloride. Using a diffusion coefficient for chloride of $2.0 \cdot 10^{-5}$ cm^2·s^{-1} , the surface of our UME (roughness factor $\simeq 10$) can be fully covered with Cl^- within approx. 20 minutes. This suggests that a significant fraction of the surface could be poisoned by chloride within the experimental time frame.

A similar argumentation was used by Katsounaros et al. who studied the effect of chloride ions, catalyst loading, and electrode rotation speed on the reduction of H_2O_2.[15] On the other hand, the cell used for the UME experiments has a rather small electrolyte volume (15 mL), such that the total number of chloride ions

present is of the same order of magnitude as the amount needed to generate a single adlayer. Finally, we consider the concentrations of other contaminants, e.g. organic carbon from the ultrapure water (<5 ppb) or nitrates from the glassware cleaning, to be too low to play a role here. Thus, the most plausible explanation is that the contamination originates from the (UME) preparation. It is noteworthy to mention that another often used supporting electrolyte, $HClO_4$, typically contains a 100-fold higher concentration of Cl^- than H_2SO_4. Although it proved to be more difficult to obtain good blank voltammetries in perchloric acid electrolytes, the best ones we obtained (Fig. 5.7) are not inferior to the ones in sulfuric acid.

5.4 Conclusions

Despite the widespread application of UMEs, the customary method of electrochemical characterization via outer sphere redox probing is insufficient if the reactivity of the electrode is studied. In this study we provide a better insight in this subject by not only measuring outer sphere redox couples, but also blank CVs and catalytic reactivity of Pt UMEs. Reactions are chosen for which plenty of data on macroelectrodes is available from the literature. To validate the UME results, the data for macroelectrodes have been measured as well for comparison.

Activity for the reduction of $[Ru(NH_3)_6]^{3+}$ and the oxidation of $FcCH_2OH$ agree very well when comparing UME responses to annealed electrodes. The onset potential is virtually identical, and a minor difference in Tafel slope can be explained by the diffusion rates for the UME being faster than experimentally possible for a macroelectrode. Also in the case of a reaction for which Pt is known to be a very good catalyst, the oxidation of N_2H_4, no significant differences between the UME and macroelectrode are observed.

However, for reactions that depend stronger on surface structure, significant differences are observed. Blank CVs of the UME do not show the well-defined hydrogen and oxide related peaks that are observed for a polycrystalline electrode. Furthermore, the normalized current in the DL region is too high, while simultaneously the oxide reduction current is too low. The CVs for methanol oxidation on Pt are similarly shaped, but the current density for the UME is about an order of magnitude lower than expected based on the electrochemical surface area. The effect is even more drastic for the reduction of nitrate, with the UME exhibiting hardly any catalytic activity. The voltammetries do not provide a means to identify a specific contaminant as no clear additional peaks were observed, although this does not imply that none were present.

Concluding, the most active sites on the UME surface seem to be blocked, with drastic consequences for reactions which depend strongly on the presence of these sites. Although the responsible process is not yet fully elucidated, there seem to be two reasonable explanations; either there is something bound so strongly to the surface (e.g. residual from the UME preparation) that it is very difficult to obtain a clean sample without flame-annealing, or diffusion is so fast that the surface easily becomes covered by trace contaminants in the electrolyte within the experimental time frame. The amount of contaminants in the used chemicals is too low to result in a significant coverage of the UME. Thus, it seems most plausible that the limited possibilities to clean the UMEs prior to use are the source of the observed effects.

Although it is uncommon to publish blank voltammetries for UMEs, our comparison to macroelectrodes shows that there is a crucial mismatch between the catalytic reactivities of these electrodes. Unfortunately, none of the widely used cleaning methods for UMEs provides an electrode cleanliness similar to flame annealing. Thus, in many cases the reactivity of UMEs will be underestimated if no proper electrochemical characterization is performed. Obviously ,this may have severe consequences for the interpretation and reproducibility of data produced using UMEs.

References

1. Zoski, C. G. Ultramicroelectrodes: Design, Fabrication, and Characterization. *Electroanalysis* **14,** 1041–1051 (2002).
2. Forster, R. J. Microelectrodes - Retrospect and prospect. *Encycl. Electrochem.* **3,** 160–195 (2002).
3. Koper, M. T. M. Structure sensitivity and nanoscale effects in electrocatalysis. *Nanoscale* **3,** 2054–2073 (2011).
4. Gilliam, R. J., Kirk, D. W. & Thorpe, S. J. Effect of electrode size on catalytic activity. *Electrochem. commun.* **9,** 875–878 (2007).
5. Gilliam, R., Kirk, D. & Thorpe, S. Dependence of catalytic activity on electrode size. *Electrochem. commun.* **9,** 2276–2279 (2007).
6. Zhou, W. P. *et al.* Morphology-dependent activity of Pt nanocatalysts for ethanol oxidation in acidic media: Nanowires versus nanoparticles. *Electrochim. Acta* **56,** 9824–9830 (2011).
7. Nesselberger, M. *et al.* The particle size effect on the oxygen reduction reaction activity of Pt catalysts: influence of electrolyte and relation to single crystal models. *J. Am. Chem. Soc.* **133,** 17428–33 (2011).
8. Chumillas, S. *et al.* Size and diffusion effects on the oxidation of formic acid and ethanol on platinum nanoparticles. *Electrochem. commun.* **13,** 1194–1197 (2011).
9. Tan, T. L., Wang, L.-L., Zhang, J., Johnson, D. D. & Bai, K. Platinum nanoparticle during electrochemical hydrogen evolution: adsorbate distribution, active reaction species, and size effect. *ACS Catal.* **5,** 2376–2383 (2015).
10. Kabbabi, A., Gloaguen, F., Andolfatto, F. & Durand, R. Particle size effect for oxygen reduction and methanol oxidation on Pt/C inside a proton exchange membrane. *J. Electroanal. Chem.* **373,** 251–254 (1994).

11. Park, S., Xie, Y. & Weaver, M. J. Electrocatalytic pathways on carbon-supported platinum nanoparticles: Comparison of particle-size-dependent rates of methanol, formic acid, and formaldehyde electrooxidation. *Langmuir* **18,** 5792–5798 (2002).
12. Rhee, C. K. *et al.* Size effect of Pt nanoparticle on catalytic activity in oxidation of methanol and formic acid: comparison to Pt(111), Pt(100), and polycrystalline Pt electrodes. *Langmuir* **25,** 7140–7 (2009).
13. Frelink, T., Visscher, W. & van Veen, J. A. R. Particle size effect of carbon-supported platinum catalysts for the electrooxidation of methanol. *J. Electroanal. Chem.* **382,** 65–72 (1995).
14. Chen, S. & Kucernak, A. Electrocatalysis under Conditions of High Mass Transport Rate: Oxygen Reduction on Single Submicrometer-Sized Pt Particles Supported on Carbon. *J. Phys. Chem. B* **108,** 3262–3276 (2004).
15. Katsounaros, I., Meier, J. C. & Mayrhofer, K. J. J. The impact of chloride ions and the catalyst loading on the reduction of H_2O_2 on high-surface-area platinum catalysts. *Electrochim. Acta* **110,** 790–795 (2013).
16. Scherson, D. A. & Tolmachev, Y. V. Impurity Effects on Oxygen Reduction Electrocatalysis at Platinum Ultramicroelectrodes: A Critical Assessment. *Electrochem. Solid-State Lett.* **13,** F1 (2010).
17. Chen, C. H. *et al.* Voltammetric scanning electrochemical cell microscopy: Dynamic imaging of hydrazine electro-oxidation on platinum electrodes. *Anal. Chem.* **87,** 5782–5789 (2015).
18. García, M. D., Marcos, M. L. & Velasco, J. G. On the mechanism of electrooxidation of hydrazine on platinum electrodes in acidic solutions. *Electroanalysis* **8,** 267–273 (1996).
19. Rosca, V. & Koper, M. T. M. Electrocatalytic oxidation of hydrazine on platinum electrodes in alkaline solutions. *Electrochim. Acta* **53,** 5199–5205 (2008).
20. Climent, V. & Feliu, J. M. Thirty years of platinum single crystal electrochemistry. *J. Solid State Electrochem.* **15,** 1297–1315 (2011).
21. Vidal-Iglesias, F. J., Arán-Ais, R. M., Solla-Gullón, J., Herrero, E. & Feliu, J. M. Electrochemical characterization of shape-controlled Pt nanoparticles in different supporting electrolytes. *ACS Catal.* **2,** 901–910 (2012).
22. Solla-Gullón, J., Rodríguez, P., Herrero, E., Aldaz, A. & Feliu, J. M. Surface characterization of platinum electrodes. en. *Phys. Chem. Chem. Phys.* **10,** 1359–73 (2008).
23. Tavares, M. C., Machado, S. A. S. & Mazo, L. H. Study of hydrogen evolution reaction in acid medium on Pt microelectrodes. *Electrochim. Acta* **46,** 4359–4369 (2001).
24. Cook, D. A. *An investigation into the electrochemical properties of nanostructured metals and their application as amperometric biosensors* PhD thesis (University of Southampton, 2005), 34–40.
25. Zhan, D., Velmurugan, J. & Mirkin, M. V. Adsorption/desorption of hydrogen on Pt nanoelectrodes: evidence of surface diffusion and spillover. *J. Am. Chem. Soc.* **131,** 14756–60 (2009).
26. Fromondi, I., Shi, P., Mineshige, A. & Scherson, D. A. In situ, time-resolved normal incidence reflectance spectroscopy of polycrystalline platinum microelectrodes in aqueous electrolytes. *J. Phys. Chem. B* **109,** 36–9 (2005).
27. Aoki, K., Zhang, C., Chen, J. & Nishiumi, T. Fabrication of glass-coated electrodes with nano- and micrometer size by means of dissolution with HF. *Electrochim. Acta* **55,** 7328–7333 (2010).
28. Chen, S. & Kucernak, A. The Voltammetric Response of Nanometer-Sized Carbon Electrodes. *J. Phys. Chem. B* **106,** 9396–9404 (2002).
29. Guo, J., Ho, C.-N. & Sun, P. Electrochemical Studies of Chemically Modified Nanometer-Sized Electrodes. *Electroanalysis* **23,** 481–486 (2011).
30. Sur, U. K., Dhason, A. & Lakshminarayanan, V. A Simple and Low-Cost Ultramicroelectrode Fabrication and Characterization Method for Undergraduate Students. *J. Chem. Educ.* **89,** 168–172 (2012).
31. Peter, L., Dürr, W., Bindra, P. & Gerischer, H. The influence of alkali metal cations on the rate of the $[Fe(CN)_6]^{4-/3-}$ electrode process. *J. Electroanal. Chem.* **71,** 31–50 (1976).
32. Beriet, C. & Pletcher, D. A microelectrode study of the mechanism and kinetics of the ferro/ferricyanide couple in aqueous media: The influence of the electrolyte and its concentration. *J. Electroanal. Chem.* **361,** 93–101 (1993).
33. Xiao, X., Pan, S., Jang, J. S., Fan, F.-R. F. & Bard, A. J. Single nanoparticle electrocatalysis: effect of monolayers on particle and electrode on electron Transfer. *J. Phys. Chem. C* **113,** 14978–14982 (2009).

34. Aldous, L. & Compton, R. G. The mechanism of hydrazine electro-oxidation revealed by platinum microelectrodes: role of residual oxides. *Phys. Chem. Chem. Phys.* **13,** 5279–5287 (2011).
35. Álvarez-Ruiz, B., Gómez, R., Orts, J. M. & Feliu, J. M. Role of the Metal and Surface Structure in the Electrooxidation of Hydrazine in Acidic Media. *J. Electrochem. Soc.* **149,** D35 (2002).
36. Herrero, E., Franaszczuk, K. & Wieckowski, A. Electrochemistry of methanol at low index crystal planes of platinum: an integrated voltammetric and chronoamperometric study. *J. Phys. Chem.* **98,** 5074–83 (1994).
37. Lai, S. C. S., Lebedeva, N. P., Housmans, T. H. M. & Koper, M. T. M. Mechanisms of carbon monoxide and methanol oxidation at single-crystal electrodes. *Top. Catal.* **46,** 320–333 (2007).
38. Housmans, T. H. M., Wonders, A. H. & Koper, M. T. M. Structure sensitivity of methanol electrooxidation pathways on platinum: an on-line electrochemical mass spectrometry study. en. *J. Phys. Chem. B* **110,** 10021–31 (2006).
39. Iwasita, T. Electrocatalysis of methanol oxidation. *Electrochim. Acta* **47,** 3663–3674 (2002).
40. Jiang, J. & Kucernak, A. Solid polymer electrolyte membrane composite microelectrode investigations of fuel cell reactions. II: voltammetric study of methanol oxidation at the nanostructured platinum microelectrode|Nafion® membrane interface. *J. Electroanal. Chem.* **576,** 223–236 (2005).
41. De Groot, M. T. & Koper, M. T. M. The influence of nitrate concentration and acidity on the electrocatalytic reduction of nitrate on platinum. *J. Electroanal. Chem.* **562,** 81–94 (2004).
42. Dima, G. E., Beltramo, G. L. & Koper, M. T. M. Nitrate reduction on single-crystal platinum electrodes. *Electrochim. Acta* **50,** 4318–4326 (2005).
43. Dima, G. E., de Vooys, A. C. A. & Koper, M. T. M. Electrocatalytic reduction of nitrate at low concentration on coinage and transition-metal electrodes in acid solutions. *J. Electroanal. Chem.* **554-555,** 15–23 (2003).
44. Greenwood, G. On the Cold-Working of Platinum Wires and the Fibrous Texture Thereby Produced. *Zeitschrift für Krist. - Cryst. Mater.* **78,** 242–250 (1931).
45. Chen, Q.-S., Solla-Gullón, J., Sun, S.-G. & Feliu, J. M. The potential of zero total charge of Pt nanoparticles and polycrystalline electrodes with different surface structure: The role of anion adsorption in fundamental electrocatalysis. *Electrochim. Acta* **55,** 7982–7994 (2010).